Available online at www.sciencedirect.com
ScienceDirect
Proceedings of the Combustion Institute 000 (2022) 1–9
Proceedings of the Combustion Institute
www.elsevier.com/locate/proci

Thermoacoustic oscillations in a can-annular model combustor with asymmetries in the can-to-can coupling

Philip E. Buschmann, Nicholas A. Worth, Jonas P. Moeck*

Department of Energy and Process Engineering, Norwegian University of Science and Technology, Trondheim, Norway

Received 6 January 2022; accepted 6 July 2022
Available online xxx

Abstract

Can-annular combustors are equipped with a set of nominally identical cans, circumferentially arranged around the shaft. Adjacent cans are coupled acoustically via a small gap at the downstream end, where the circular cross-section transitions into the annular turbine inlet. Recent experimental and theoretical work has shown that the coupling strongly affects thermoacoustic system stability and, hence, may give rise to damaging pressure oscillations that originate from a constructive interference of pressure waves and heat release rate fluctuations. A laboratory-scale can-annular combustor has been operated with premixed CH_4–H_2–air mixtures to study these instabilities. The combustor consists of eight identical cans, connected acoustically to their respective neighbours via size-adjustable side branches; the latter allow for a variation of the coupling strength. New experimental results are presented in which five asymmetric sets of coupling strengths are investigated and compared to a previously studied symmetric configuration. The sets are chosen such that the symmetry is gradually reduced until a fully asymmetric configuration is realized. The perturbations affect the observed mode type, frequency of oscillation and the pressure amplitude distribution over the eight cans. The perturbations via the can-to-can couplings do not trigger mode localization. The symmetric configuration considered previously, shows activity in an azimuthal mode of third and fourth order, with unsteady switching between the two. The mode shape is characterised through novel phase-averaged OH^* chemiluminescence images capturing all eight cans.

Keywords: Can-annular combustor; Thermoacoustics; Azimuthal mode; Eigenvalue cluster; Symmetry breaking

1. Introduction

Combustion chambers for applications in stationary power generation are operated under lean premixed conditions to ensure a clean combustion process with low NOx emissions. Lean premixed flames are especially vulnerable to an unstable coupling between heat release rate and acoustic waves, which can trigger undesirable dynamic phenomena, most prominently thermoacoustic instability [1–5]. The associated large amplitude pressure oscillations prevent safe operation and, thus, limit the operating range of the engine. Therefore, insight into the occurrence and manifestation of these

* Corresponding author.
E-mail address: jonas.moeck@ntnu.no (J.P. Moeck).

https://doi.org/10.1016/j.proci.2022.07.060
1540-7489 © 2022 Published by Elsevier Inc. on behalf of The Combustion Institute.

instabilities is required to develop predictive modeling methods and effective mitigation strategies.

In stationary gas turbines, a well-established combustor design consists of a number N of can combustors (usually 8 to 16) arranged around circumferentially. From a development perspective, this design has many advantages over an annular combustion chamber with respect to cutting costs and development time: air–fuel mixing, flashback and blow-off sensitivity can be studied on a single can. However, this design exhibits special types of thermoacoustic phenomena. These are caused by a coupling between adjacent cans that exists due to the fact that all circular can cross-sections need to be merged to an annular gap towards the turbine inlet, which is annular. By merging these two different cross-sections, a small gap between adjacent cans – the acoustic cross-talk (XT) – results. Via the XTs acoustic waves can propagate between adjacent cans and exhibit thermoacoustic phenomena that cannot be observed by studying a single, isolated can combustor. As the cross-talk area is typically small, the coupling between the cans is considered to be weak [6].

When considering the thermoacoustic dynamics of a can-annular combustor, a common spectral characteristic is the occurrence of mode clusters, different from their annular counterparts. The emergence of these eigenvalue clusters can be understood as follows. Assume that the XT area, and thus the strength of the acoustic coupling, is described by a non-dimensional parameter ε, which is small because the coupling is weak. For closed XTs $\varepsilon = 0$; then all combustors can oscillate in a standalone, isolated fashion without being synchronized. The system exhibits an N-fold degenerate eigenvalue, where N is the number of combustors cans. As the XT area is opened, $\varepsilon > 0$, this N-fold degenerate eigenvalue splits into distinct azimuthal modes [7] of various azimuthal mode orders m, which, for the low-frequency regime considered here, take values

$$m \in \left\{0, 1, \ \ldots \ \frac{N}{2} - 1, \frac{N}{2}\right\}, \tag{1}$$

for even m and

$$m \in \left\{0, 1, \ \ldots \ \frac{N-1}{2}\right\}, \tag{2}$$

for odd m. For even m, modes of lowest order $m = 0$ are commonly referred to as push-push modes (all cans oscillate in phase) and modes of highest order $m = N/2$ as push–pull modes (adjacent cans oscillate in phase opposition). For even m, modes $m = 1, \ldots, N/2 - 2$ are twofold degenerate and can be of standing or spinning type. Since the coupling through the XT is small, $\varepsilon \ll 1$, and the post-split modes remain in a narrow frequency band and form a mode cluster [6]. As stated by [6], the case of odd m is not found in applications for manufacturing reason. The gas turbine casing consists of two halves and for odd m a bisecting plane would intersect one can combustor, which is impractical.

Perturbations in the coupling strength between adjacent cans can occur naturally in industrial can-annular combustors. Asymmetries in nominally highly symmetric annular or can-annular combustors may also be introduced deliberately to mitigate undesirable dynamics [8]. Manufacturing imperfections in the mixture supply of individual cans can affect the mean gas properties that exit the cans towards the turbine stage. These can change the acoustic response of the cross-talk [21] and affect the coupling strengths. Therefore, it is of interest to study these effects in the controlled environment of a laboratory-scale combustor. For can-annular combustors, asymmetric perturbations of the coupling strength have not been studied in laboratory experiments previously.

In a series of three papers, Moon et al. [9–11] have studied thermoacoustic instabilities in can-annular combustors with four cans and have investigated the effect of an asymmetric distribution of the equivalence ratios among the cans. The work by Moon et al. revealed clustered modes with azimuthal orders obeying Eq. (1) and showed that degenerate modes of standing and spinning type exist. Depending on the asymmetries in the equivalence ratio distribution, with cans having pairwise or alternating the same equivalence ratio, different modes are triggered.

Moon et al. furthermore observe mode localization. Here, 'localization' refers to the fact that a mode is only active in few cans, while the remainder remain silent or show only small amplitude oscillations [12]. This effect is well-known for systems composed of weakly coupled, nominally identical subcomponents [13]. An unstable localized mode is a severe problem for a can-annular combustor since the instability can only be recorded by having pressure sensors in all cans. Mode localization is favored in conditions where closely neighbouring eigenvalues, such as the clusters found in can-annular combustors, are exposed to asymmetric perturbations (in the structural context typically referred to as 'disorder') [14,15]. However, the type of perturbation is important. As will be detailed in the results section, a perturbation of the can-to-can coupling – as is considered in the present work – is not expected to trigger localization. In [12] it is shown that mode localization can also exist in a can-annular setup with nominally symmetric cans. A perturbation to the systems symmetry can then only be related to natural imperfections in the set up and mixture supply or is introduced through the nonlinearity in the flame response. The latter naturally causes an asymmetry in the mean field at finite oscillation amplitudes.

In previous work [16], a nominally symmetric can-annular combustor was studied, where the cross-talk strength was decreased, while maintaining a symmetric distribution in the set up. The re-

Please cite this article as: P.E. Buschmann, N.A. Worth and J.P. Moeck, Thermoacoustic oscillations in a can-annular model combustor with asymmetries in the can-to-can coupling, Proceedings of the Combustion Institute, https://doi.org/10.1016/j.proci.2022.07.060

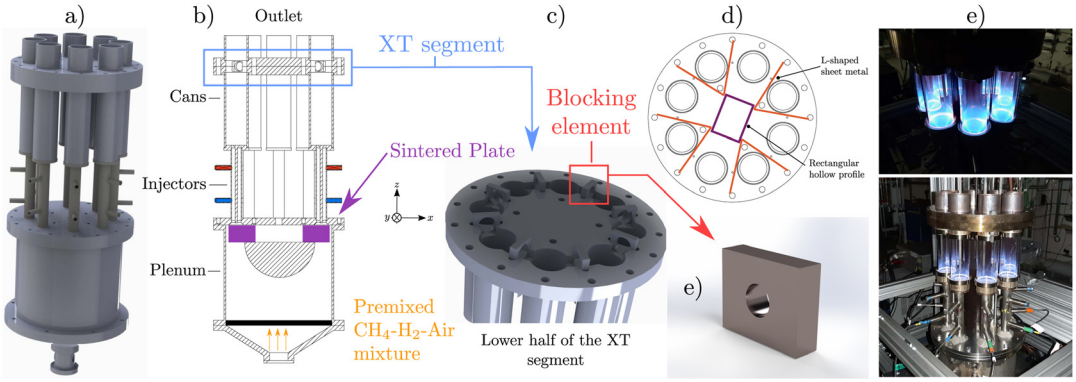

Fig. 1. a) Computer rendering of the can-annular rig. The sheet metal plates mounted at the outlet are not depicted. b) Axial cut through the rig. All eight cans are fed with the same mixture via the plenum. The sintered plate that decouples the plenum acoustically is depicted in purple. Pressure transducers are mounted in the lower ports (blue), while the upper ones (red) are blocked. c) Lower half of the XT section with the blocking stones mounted. An identical plate is mounted from above. Different blocking elements can be inserted to vary the strength of the acoustic coupling. e) Rendering of a blocking element with a central bore. e) Pictures of the combustor in operation with flames sitting in quartz tubes.

sults show that a reduction in coupling strength lowers the frequencies of all observed modes, which confirms earlier theoretical results from [6] and [7]. In addition, a weaker coupling resulted in lower mean pressure amplitudes in all cans. All configurations showed activity in azimuthal modes of third and fourth order, but as the coupling strength is decreased, the can-annular combustor increasingly favors a push–pull instability over a standing mode of third order, which is encountered for strong coupling. In the present work, the nominally symmetric case in [16] serves as a reference. The nominal symmetry is perturbed by inserting blocking elements of different diameter into the cross-talk to vary the strength of the acoustic coupling. Care is taken to ensure that these changes are conducted in a systematic matter, whereby configurations with increasingly lower symmetry are investigated until full asymmetry is reached. This is the first experimental work using a can-annular combustor, where such a perturbation is considered.

2. Experimental setup

The can-annular model combustor is depicted in Fig. 1. It consists of eight cans that are fed from a shared plenum with unburned fuel–air mixture. At the inlet of the injectors, a sintered plate of type SIKA-B200 with a porosity of 51% and pore size 124 μm is mounted. The plate is acoustically highly reflective and significantly reduces acoustic coupling between the cans via the plenum. Bluff-bodies are used as flame holders in every can. At the downstream end of the cans, a coupling segment – the XT section – permits acoustic waves to travel between adjacent cans. The strength of the XT-coupling is adjusted by inserting cuboidal blocking elements with different bore holes, see Table 1 for the dimensions. At the outlet of the cans, sheet metal plates are mounted to prohibit acoustic communication via the ends and, thus, confine the acoustic communication to the XT-coupling. The geometric dimensions and acoustic properties of the sintered plate, that were determined with the multi-microphone method, can be found in [16]. The open can outlets approximately impose an acoustic pressure node. This differs from the acoustic boundary condition found in gas turbine combustors, where the turbine inlet approximately imposes an acoustic velocity node. However, the latter cannot be realized in an atmospheric rig, and we assume that the qualitative effect of introducing asymmetries in the XT section is similar.

The combustor is operated with perfectly premixed CH_4–H_2–air mixture. The thermal power for each can is 8.3kW at an equivalence ratio of $\phi = 0.85$ and with a hydrogen content of 8% by power (approximately 20% by volume). An Optris CTlaser 3MHCF4 pyrometer is aimed at the outlet of one can to measure the temperature. After one experimental run a new one is started once the outlet temperature drops to 350°C to ensure repeatability. An experimental run has a duration of 60s.

Pressure signals are recorded with a 24-bit DAQ system (NI model 9174) and eight Kulite (XCS-093-05D) pressure transducers. The sampling frequency is $f_s = 51.2$kHz and the signals are amplified with a FE-579-TA Bridge Amplifier from FYLDE set to a gain of 300 and using a built-in analogue low-pass filter with cut-off at 20kHz. The pressure spectra are estimated using Welch's method, where the pressure signals are binned into segments of length 400ms, an overlap of 75% is used, and the segments are zero-padded to double the size. Spectrograms are computed with short-

Please cite this article as: P.E. Buschmann, N.A. Worth and J.P. Moeck, Thermoacoustic oscillations in a can-annular model combustor with asymmetries in the can-to-can coupling, Proceedings of the Combustion Institute, https://doi.org/10.1016/j.proci.2022.07.060

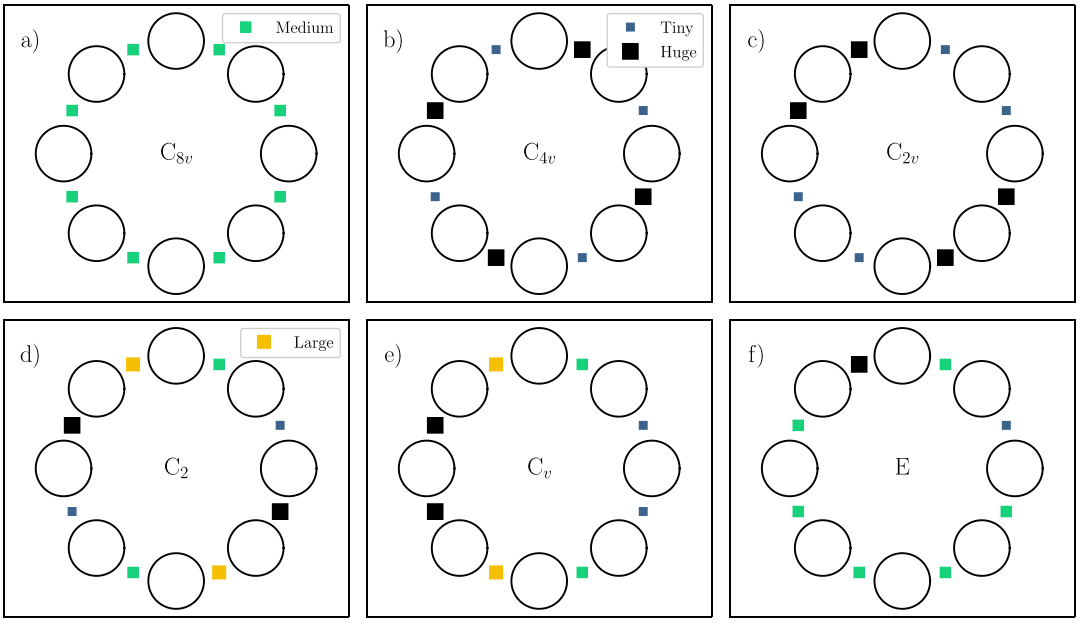

Fig. 2. Schematic top view of the can-annular model combustor with the patterns of blocking elements that are installed to lower the symmetry. The black circles represent the cans and the colored squares the blocking elements. For the dimensions of the blocking elements see Table 1. The group name in Schönfliess notation is given in the center of each configuration.

time Fourier transforms, using the same parameters as for Welch's method. Amplitudes are calculated as the RMS value of the signal and, if data is filtered using the Fourier transform, the filter limits are given in the results section. In order to extract information about the modal orders m, the pressure signals are projected onto a standing wave basis. The projection returns modal coefficients a_m^s and a_m^c for the circumferential sine and cosine basis, respectively. For details on the modal projection, see [16] and references therein.

In order to visualize a specific mode, a Photron SA1.1 CMOS camera is mounted downstream of the setup, in an overhead configuration. The setup is similar to the one shown in [17]. In conjunction with a LaVision Intensified Relay Optics unit and a Cerco 2178 UV lens equipped with a D20-VG0035942 filter (centre wavelength 310nm, full width half maximum 10nm), the camera images the OH^* chemiluminescence intensity emitted from the zone of heat release. Images are recorded at 10kHz and for one second only, due to the limited memory size on the camera. Therefore, a recording of major parts of an experimental run that includes transient behaviour was not possible.

3. Asymmetries in the can-to-can coupling strength

Fig. 2 depicts, in a schematic way, the different configurations that are investigated. The nominally symmetric configuration in Fig. 2a) is perturbed by inserting heterogeneous sets of blocking elements. A perturbation of the reactant mixtures is not feasible in the current setup since all cans are fed from a shared plenum.

Table 1
Dimensions of the blocking elements which are employed to adjust the strength of the coupling between adjacent cans. d is the diameter of the bore in each blocking element and A_{XT} and A_{can} are the areas of the XT ($\pi d^2/4$) and of the cans, respectively.

Name	Tiny	Medium	Large	Huge
d in mm	9.4	16.2	18.7	20.0
A_{XT}/A_{can}	0.05	0.15	0.20	0.23

In the center of each geometry, the name of the associated symmetry group [18] is given, which is simply used as a label for the present purpose. The names follow the Schönfliess notation. Starting from Fig. 2a), the symmetry is gradually lowered until full asymmetry is attained with the geometry in Fig. 2f). Here, a 'lower' symmetry refers to the fact that fewer spatial transformations leave the configuration invariant. For instance, there are 8 rotations (by multiples of $2\pi/8$) and 8 reflections that leave the combustor configuration C_{8v} invariant. The subscript 8 in C_{8v} refers to both of these. Conversely, only two such rotations and reflections exist for C_{2v}. Hence, C_{8v} consists of 16 elements, while that number is 8,4,2,2 and 1 for C_{4v}, C_{2v}, C_2, C_v and E, respectively.

Please cite this article as: P.E. Buschmann, N.A. Worth and J.P. Moeck, Thermoacoustic oscillations in a can-annular model combustor with asymmetries in the can-to-can coupling, Proceedings of the Combustion Institute, https://doi.org/10.1016/j.proci.2022.07.060

The theory of symmetry groups [18] is useful to determine all possible intermediate states between maximum symmetry (C_{8v}) and full asymmetry (E), that can be realized in this experiment by geometric means. In the language of symmetry groups, C_{4v}, C_{2v}, C_2 and C_v are subgroups of C_{8v}. The symmetry structure of the configuration is essential in the context of thermoacoustic oscillations because it determines which modes are degenerate.

The symmetry groups in Fig. 2 can be realized using different geometries, e.g. via different sets of blocking elements. For instance, C_{8v} can also be realized by employing any other blocking element besides 'Medium'. In particular, the fully asymmetric configuration E can be realized in a number of different ways, e.g. by placing the 'Tiny' blocking element in any other slot except opposite of 'Huge'. More possibilities are easily envisaged.

4. Results and discussion

Fig. 3 shows the pressure spectra and the amplitudes of the modal coefficients for all cases. The case C_{8v} is the one labeled 'Medium' in [16] for configuration SP (sintered plate). All configurations show activity in a lower-frequency cluster and a higher-frequency cluster. For every case, all pressure transducers show the same frequency peaks, but for C_v and E, the amplitudes differ significantly. As Fig. 3a) shows, changes of the geometry have little effect on the frequencies in the lower cluster but cause a significant spread in the higher-frequency cluster. Only C_2 shows a clearly offset secondary peak.

In the lower-frequency cluster, modes are exclusively of push–push type, see Fig. 3f). In the higher-frequency cluster, primarily a push–pull mode is active, with some activity of an $m = 3$ mode for some of the configurations, see Fig. 3g). Fig. 3b) and c) show the same time series of case E for a short window in time but bandpass filtered around the frequencies of the lower and the upper cluster, respectively. As Fig. 3b) depicts, all cans oscillate in phase and a push–push mode is present. Conversely, Fig. 3c) shows that in the upper cluster neighbouring modes oscillate out of phase – indicative of a push–pull mode. The histograms of the phase difference in Fig. 3d) and e) also support this, by showing the in-phase and out-of-phase character of adjacent cans, respectively. Case E is representative for the other cases to show the different behaviour in the two clusters. However, all cases with lower symmetry show less activity in the $m = 3$ mode than the unperturbed case C_{8v}. In fact, there is a transient switching between modes of order $m = 3$ and $m = 4$. A short-time Fourier transform (STFT) that illustrates this behaviour for two windows in time is shown in Fig. 4a) and b).

To characterize the simultaneous occurrence of two modes for the symmetric configuration C_{8v}, a joint probability density function (PDF) of their amplitudes is shown in Fig. 4c) and d) for a_4^c with a_3^c and a_3^s. Frames c) and d) in Fig. 4 show that the oscillation in the $m = 4$ mode is predominantly accompanied by small-amplitude oscillations in both a_3^c and a_3^s. A higher-amplitude oscillation (1500Pa) in a_4^c tends to occur jointly with a_3^s, while a lower amplitude (1000Pa) one is correlated with a_3^c. For a_3^c an oscillation at a secondary, higher amplitude also occurs, albeit more rarely during the recorded experiment. Conversely, an oscillation of a_3^s at 450Pa is only observed if a_4^c is significantly weaker (500Pa). The difference is surprising since one would expect a_3^c and a_3^s to exhibit similar characteristics in a symmetric configuration. However, the nonlinearity in the flame response introduces asymmetries in the can dynamics even in a nominally symmetric system.

To illustrate how an $m = 3$ mode manifests itself in a can-annular combustor with eight cans, Fig. 5 depicts the phase-averaged OH^* chemiluminescence images corresponding to the heat release rate fluctuations. No camera data was recorded at the exact time, when a standing mode $m = 3$ is active during the experiment for configuration C_{8v}. Hence, the result of a run with the same operating conditions but with blocking elements 'Open' installed are shown, where such an $m = 3$ instability is recorded. The oscillation frequency obtained from the camera data matches with the frequency of an $m = 3$ mode according to the pressure data.

According to the oscillation patterns, cans 45°, 180° and 270° clearly oscillate in phase. In antiphase to this trio is only can 225°. Cans at 0° and 90° are possibly in phase with 225°, but the experimental evidence is not strong for the former and weak for the latter. This pattern may imply that two nodal lines are located in the XTs between 180° – 225° (and opposite between 0° – 45°), and 225° – 270° (and opposite between 45° – 90°). Since the oscillation amplitudes are very small in the cans at 135° and 315°, the third and final nodal line should be located in these two. If the nodal lines are oriented in this fashion, the angles between them would not be equal. The alignment would be consistent with work of [19] that proves for finite-amplitude oscillations in annular combustion chambers that the orientation of the nodal lines is not arbitrary but needs to pass through the burners or in-between burners.

From Fig. 3h) it can be seen that the cases C_{4v}, C_{2v} and C_2 are very similar in pressure amplitudes and exhibit little variation over the circumference. In fact, the observed pressure amplitudes are slightly less than for the baseline case C_{8v}. In contrast, the cases C_v and E in Fig. 3i) show higher amplitudes in the cans at 270°, 315° and 0°. This can also be observed in the pressure time series of Fig. 3c). The observed pressure amplitude is almost twice as high as in the remaining cans. For both configurations, the highest overall value is reached

Please cite this article as: P.E. Buschmann, N.A. Worth and J.P. Moeck, Thermoacoustic oscillations in a can-annular model combustor with asymmetries in the can-to-can coupling, Proceedings of the Combustion Institute, https://doi.org/10.1016/j.proci.2022.07.060

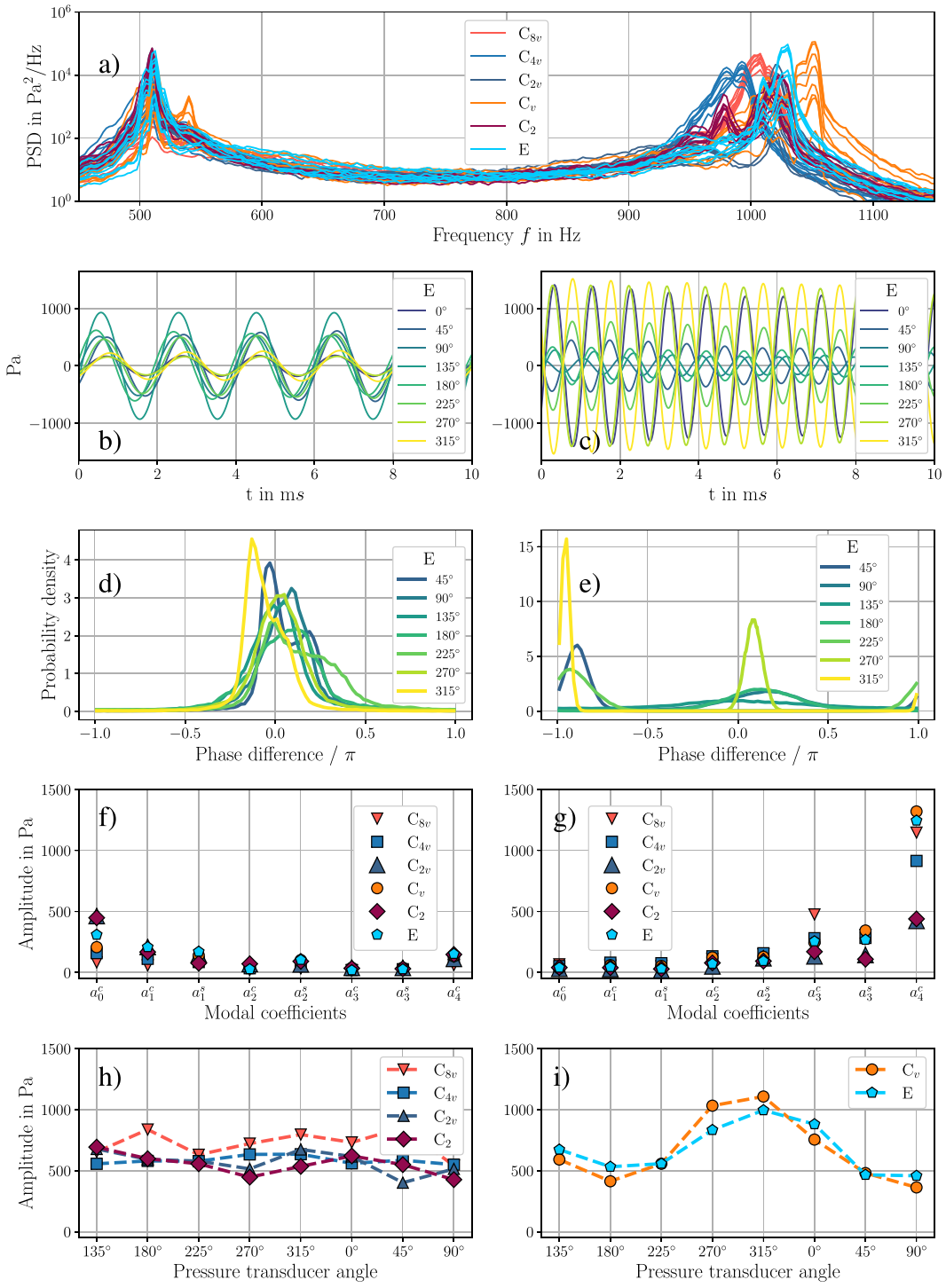

Fig. 3. a) Pressure spectra for all cases and all eight pressure transducers per case. b) & c) Selected window in the pressure time series after 20 seconds of recording for case E. Signals from all cans are depicted and bandpass filtered in the range $f_{\text{filt}} \in [480, 540]$ Hz for b) and $f_{\text{filt}} \in [900, 1150]$ Hz for c). d) & e) Histogram of the phase difference with respect to the signal in the can at 0° for case E for the entire duration of recording. f) & g) RMS amplitudes of the modal coefficients when the pressure signals are bandpass filtered in the range $f_{\text{filt}} \in [480, 540]$ Hz for f) and $f_{\text{filt}} \in [900, 1150]$ Hz for g). h) & i) RMS pressure amplitudes in the individual cans.

Please cite this article as: P.E. Buschmann, N.A. Worth and J.P. Moeck, Thermoacoustic oscillations in a can-annular model combustor with asymmetries in the can-to-can coupling, Proceedings of the Combustion Institute, https://doi.org/10.1016/j.proci.2022.07.060

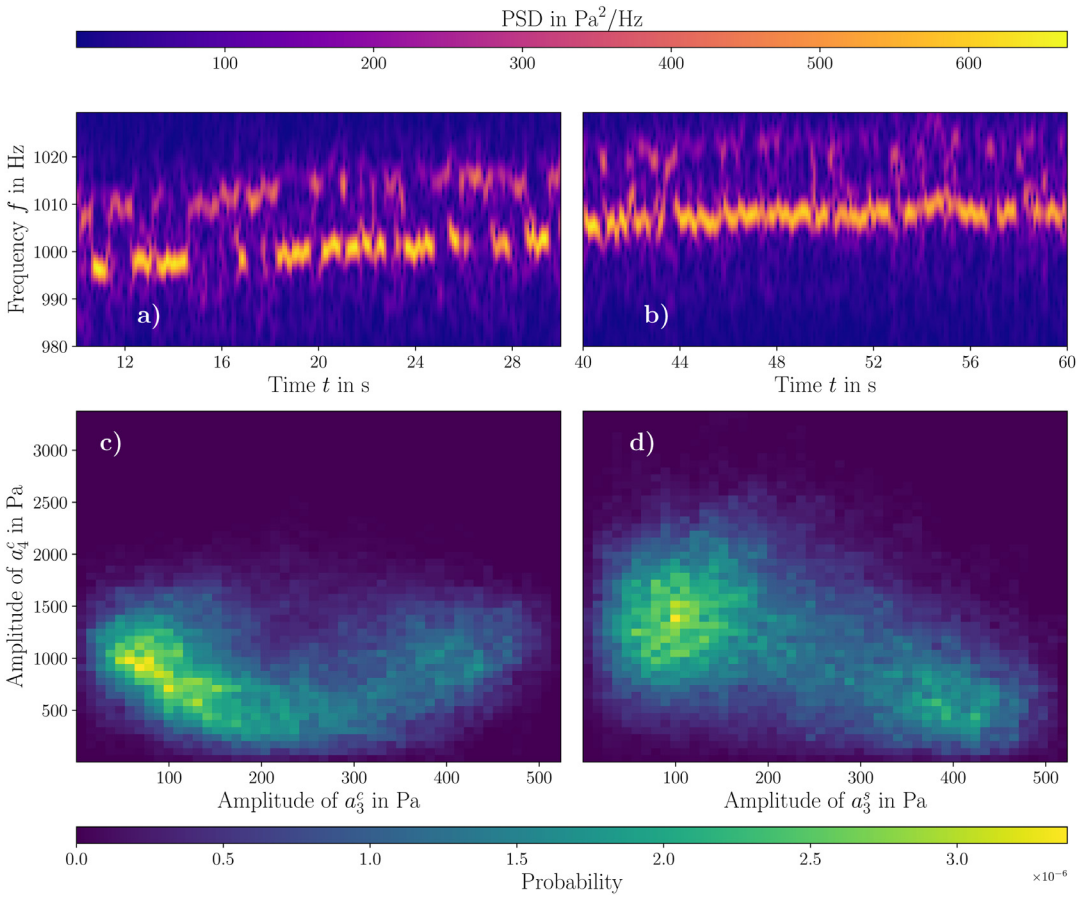

Fig. 4. a) and b) STFT of the pressure signal for the pressure transducer at 180° for two windows of 20s during the 60s operation. The lower frequency is of an $m = 3$ mode and the higher frequency of an $m = 4$ mode. During operation the test rig heats up which causes a gradual drift towards higher frequencies. c) and d) Joint PDF for C_{8v} of mode $m = 4$ with the c) cosine and d) sine components of mode $m = 3$ for the entire experimental run of 60s.

in the 315° can. Even though the cases C_{8v}, C_v and E show similar amplitudes in the $m = 4$ component, the amplitude distributions over the circumference are very different.

The employed perturbations of the coupling strength did not trigger a mode localization – the variation in amplitude over the circumference for C_v and E is not sufficient to classify it as such. This is expected, since systems of weakly coupled oscillators are mainly vulnerable to mode localization if the properties of the individual oscillators are perturbed [14,15,20] and not the coupling strength – as conducted in this work. For a can combustor the obvious choice would be a change in operating conditions to modify the flame response. This strategy has been pursued by Moon et al. [10,11], where changes alone in the equivalence ratios of individual cans trigger mode localizations. However, the phenomenon is also observed under purely symmetric operating conditions [12].

The cases of lower symmetry for which experiments have been performed are not the only subgroups of C_{8v}. The are two more subgroups, viz. C_8 and C_4, that cannot be realized in the present experiment due to the employed bluff-bodies. Both of these groups only contain rotations, which are 8 rotations (by $2\pi/8$) for C_8 and 4 (by $2\pi/4$) for C_4. With bluff-bodies, it is reasonable to assume that the flow field in every combustion chamber exhibits a reflection symmetry. As a consequence, no combination of blocking elements facilitates a removal of only the reflection symmetry, while maintaining the rotational symmetry. By using swirlers as flame holders, the reflection symmetry of the cans is removed due to the resulting flow field. A setup with eight swirlers and identical blocking elements in all slots would exhibit C_8 symmetry. However, this would require a comparison of results between bluff-body and swirl-stabilized flames, which is not considered since the responses of these flames to

Please cite this article as: P.E. Buschmann, N.A. Worth and J.P. Moeck, Thermoacoustic oscillations in a can-annular model combustor with asymmetries in the can-to-can coupling, Proceedings of the Combustion Institute, https://doi.org/10.1016/j.proci.2022.07.060

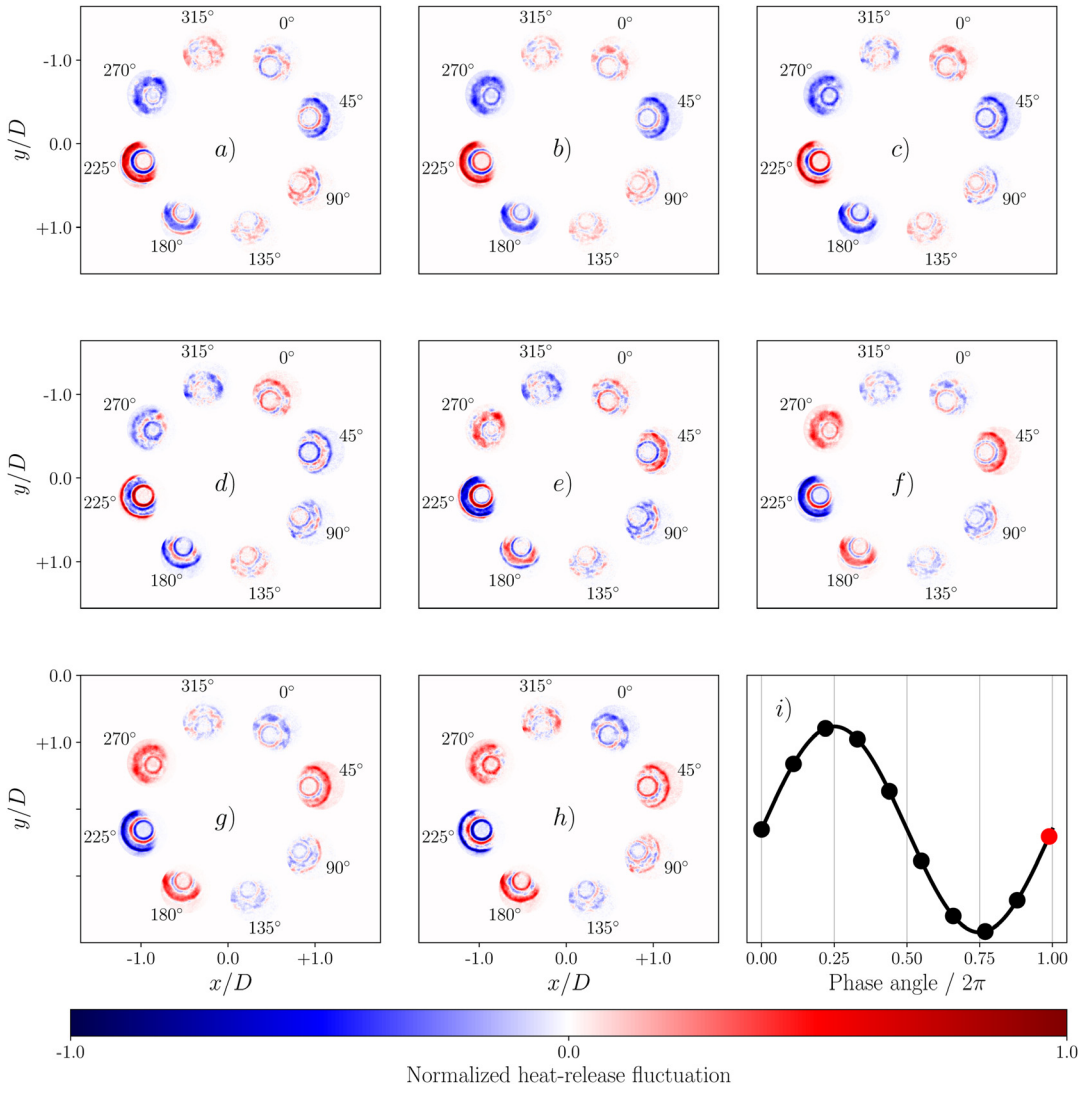

Fig. 5. a) – h) Phase-averaged OH* chemiluminescence images visualizing the heat release rate perturbation associated with an $m = 3$ mode from a downstream view. The experimental data is from a run with blocking elements 'Open' in all XT gaps. i) Schematic depiction of the phase angles from a) to h), as dictated by the available data. The red dot represents the final image, which is not shown since the angle is very close to the one in a).

acoustic perturbations are very different. The same argument holds for C_4.

5. Conclusion

The nominal symmetry of a model can-annular model combustor is perturbed by introducing asymmetries in the can-to-can coupling strength. Even though the adjustments are minor, shifts in frequencies and modal structure are observed. All perturbations show a push–pull mode, while the unperturbed reference case exhibits a third order mode in addition to a push–pull mode. For the first time, the mode shape of a third-order azimuthal mode in a can-annular combustor is visualized using phase-averaged OH* chemiluminescence images. The findings show that a perturbation in the weak coupling can affect the modal structure, depending on the perturbation, trigger different pressure amplitude distributions over the circumference. For this combustor, a perturbation in the weak coupling is insufficient to trigger mode localization.

Future work will investigate if different geometrical implementations of the asymmetric configuration E have an effect on the observed instabilities and study the effect of even weaker can-to-can

Please cite this article as: P.E. Buschmann, N.A. Worth and J.P. Moeck, Thermoacoustic oscillations in a can-annular model combustor with asymmetries in the can-to-can coupling, Proceedings of the Combustion Institute, https://doi.org/10.1016/j.proci.2022.07.060

coupling. Perturbations in the inlet conditions of each can will be considered to systematically assess the susceptibility to localization. The case of odd m is not strictly relevant for practical applications, but can give new insights into the modal dynamics. Therefore, future work will re-configure the can-annular combustor into such an odd number of cans and investigate the dynamics.

Declaration of Competing Interest

The authors declare that they have no known competing financial interests or personal relationships that could have appeared to influence the work reported in this paper.

References

[1] Overview of combustion instabilities in liquid-propellant rocket engines. Chap. 1 In: Yang V, Anderson WE, editors: Liquid Rocket Engine Combustion Instability, volume 169, Progress in Astronautics and Aeronautics, 1995.
[2] A.P. Dowling, S.R. Stow, Acoustic analysis of gas turbine combustors, J. Propul. Power 19 (5) (2003) 751–764.
[3] S. Ducruix, T. Schuller, D. Durox, S. Candel, Combustion dynamics and instabilities: Elementary coupling and driving mechanisms, J. Propul. Power 19 (5) (2003) 722–734.
[4] Combustion Instabilities in Gas Turbine Engines, in: T.C. Lieuwen, V. Yang (Eds.), Prog. Astronaut. Aeronaut., volume 210, AIAA, Inc., 2005.
[5] LieuwenTim C, Unsteady combustor physics, Cambridge University Press, 2021.
[6] G. Ghirardo, C. Di Giovine, J.P. Moeck, M.R. Bothien, Thermoacoustics of can-annular combustors, J. Eng. Gas Turbines Power 141 (1) (2019) 011007.
[7] J.G. von Saldern, J.P. Moeck, A. Orchini, Nonlinear interaction between clustered unstable thermoacoustic modes in can-annular combustors, Proc. of the Comb. Inst. 38 (4) (2020) 6145–6153.
[8] M. Bothien, N. Noiray, B. Schuermans, Analysis of azimuthal thermo-acoustic modes in annular gas turbine combustion chambers, J. Eng. Gas Turbines Power 137 (2015). 061505 (8 pages)
[9] K. Moon, H. Jegal, C. Yoon, K.T. Kim, Cross-talk-interaction-induced combustion instabilities in a can-annular lean-premixed combustor configuration, Combust. Flame 220 (2020) 178–188.
[10] K. Moon, C. Yoon, K.T. Kim, Influence of rotational asymmetry on thermoacoustic instabilities in a can-annular lean-premixed combustor, Combust. Flame 223 (2020) 295–306.
[11] K. Moon, Y. Choi, K.T. Kim, Experimental investigation of lean-premixed hydrogen combustion instabilities in a can-annular combustion system, Combust. Flame (2021) 111697.
[12] G. Ghirardo, J. Moeck, M.R. Bothien, Effect of noise and nonlinearities on thermoacoustics of can-annular combustors, J. Eng. Gas Turbines Power 142 (4) (2020) 041005.
[13] C. Hodges, Confinement of vibration by structural irregularity, J. Sound Vib. 82 (3) (1982) 411–424.
[14] C. Pierre, Mode localization and eigenvalue loci veering phenomena in disordered structures, J. Sound Vib. 126 (3) (1988) 485–502.
[15] C. Pierre, P.D. Cha, Strong mode localization in nearly periodic disordered structures, AIAA J. 27 (2) (1989) 227–241.
[16] P.E. Buschmann, N.A. Worth, J.P. Moeck, Experimental study of thermoacoustic modes in a can-annular model combustor, SoTiC 2021 - Symposium on Thermoacoustics in Combustion: Industry meets Academia, 2021.
[17] H.T. Nygård, Experimental Measurement of Flame Describing Functions in an Azimuthally Forced Annular Combustor, NTNU, Trondheim, Norway, 2021 Ph.D. thesis.
[18] T. Inui, Y. Tanabe, Y. Onodera, Group theory and its applications in physics, volume 78, Springer Science & Business Media, 2012.
[19] G. Ghirardo, M. Juniper, J.P. Moeck, Weakly nonlinear analysis of thermoacoustic instabilities in annular combustors, J. Fluid Mech. 805 (2016) 52–87.
[20] M. Triantafyllou, G. Triantafyllou, Frequency coalescence and mode localization phenomena: a geometric theory, J. Sound Vib. 150 (3) (1991) 485–500.
[21] A. Orchini, T. Pedergnana, P.E. Buschmann, J. P. Moeck, N. Noiray, Reduced-order modelling of thermoacoustic instabilities in can-annular combustors, J. Sound. Vib. 526 (2022).

Please cite this article as: P.E. Buschmann, N.A. Worth and J.P. Moeck, Thermoacoustic oscillations in a can-annular model combustor with asymmetries in the can-to-can coupling, Proceedings of the Combustion Institute, https://doi.org/10.1016/j.proci.2022.07.060